# Simultaneous optical and infrared polarization measurements of blazars

C. Brindle and J. H. Hough Hatfield Polytechnic Observatory, Bayfordbury House, Hertford, Herts SG13 8LD

J. A. Bailey Anglo-Australian Observatory, PO Box 296, Epping, NSW 2121, Australia

D. J. Axon University of Manchester, Nuffield Radio Astronomy Laboratories, Jodrell Bank, Macclesfield, Cheshire SK11 9DL

A. R. Hyland Mount Stromlo and Siding Spring Observatories, Private Bag, Woden, ACT 2606, Australia

Accepted 1986 March 19. Received 1986 February 24; in original form 1985 November 5

**Summary.** We present measurements of the polarization and flux of a sample of 28 blazars (21 BL Lacs and 7 OVV quasars) at optical and near-infrared wavelengths, with repeated observations for some objects. For 20 objects, these are the first reported polarization measurements in either the optical or infrared, and for most of them the first simultaneous measurements at these wavelengths.

Out of a total of 42 observations we find a spectral dependence of polarization level and position angle, although not necessarily occurring together, on 15 occasions.

As in earlier work, we find that the levels of polarization in the infrared are generally equal to, or lower than, those in the optical, although for some objects with low levels of polarization (P < 10 per cent), the polarization in the infrared can exceed that in the optical. Large wavelength dependences of polarization, in which the polarization increases with decreasing wavelength, were observed for both high and modest ( $P \sim 10$  per cent) values of the optical polarization of an object. Thus the trend of increasing wavelength dependence of polarization with increasing polarization, found from earlier polarization studies, is less significant.

Marked variations in the wavelength dependence of polarization were observed on consecutive nights for some of the objects. Models consisting of two synchrotron sources, with different spectral indices, can satisfactorily account for the wavelength dependence of both the polarization and flux.

#### 1 Introduction

Blazars show the most rapid variability of active galactic nuclei, with significant changes in brightness and polarization occurring on time-scales of typically one day (Angel et al. 1978;

Moore & Stockman 1981, 1984; Moore et al. 1982; Brindle et al. 1985 and references therein). The high polarization and rapid variability are generally interpreted as being due to incoherent synchrotron radiation produced close to a massive black hole. OVV quasars are distinguished from BL Lacs by the presence of strong emission lines, as in 'normal' quasars (Stockman, Moore & Angel 1984). Angel & Stockman (1980) have reviewed the polarization properties of blazars and a review of the optical and infrared polarization properties of all active galactic nuclei has recently been given by Martin (1985). Moore & Stockman (1984) have compared the properties of OVV quasars and low-polarization quasars.

The wavelength dependence of polarization for blazars is still poorly determined. Since the dependence is often weak measurements are needed over a wide wavelength range, and in addition the measurements must be made over a short time interval so as to minimize the effects of variability.

Nordsieck (1976) attempted to explain the wavelength dependence of polarization by a change in the slope of the electron spectrum with energy, but in most cases the effect is small. More recently Puschell et al. (1983) and Holmes et al. (1984a, hereafter HBIW) have proposed that the superposition of different synchrotron sources can account for a spectral dependence of both the level and the position angle of polarization. Björnsson (1985) has shown how a large wavelength dependence in both the degree and position angle of polarization can arise from a single synchrotron component, and suggests that the multi-component models are probably only an approximation to a single, complex synchrotron component.

The aim of our programme was to measure the polarization in one optical and one infrared band, usually R and H, for as many blazars as possible. Where a wavelength dependence was observed further measurements were made in several other bands from U to K (0.36–2.19  $\mu$ m).

In Section 2 we give details of the observations and the data are presented in Table 1. In Section 3 there is a discussion of some of the statistical properties of the data and in Section 4 we discuss some simple models to account for the wavelength dependence of flux and polarization seen in some of the objects.

#### 2 Observations

Most of the observations presented here were made at the 3.9-m Anglo-Australian Telescope (AAT), on two observing runs. The first one was on the nights of 1982 December 24 and 25, and the second between 1984 August 15 and 21. In addition, some data acquired with the AAT on other dates are presented and also some data acquired with the 3.8-m United Kingdom Infrared Telescope (UKIRT) at Mauna Kea.

On all occasions the Hatfield dual-beam polarimeter was used to make simultaneous observations at one optical and one infrared waveband. The configuration of the polarimeter was slightly different to that described by Bailey & Hough (1982). The polarization modulation was achieved by continuously rotating a superachromatic half-wave plate, followed by a Foster beam-splitting prism. The straight-through beam was directed to a cooled GaAs photomultiplier and the side beam was directed to the infrared Photometer Spectrometer (IRPS) at the AAT and to the two-channel InSb infrared photometer at UKIRT. Polarization measurements were calibrated using a Glan prism which could be inserted ahead of the rotating waveplate. Polarization standards were also used to check the measured level of polarization and to establish the zero of the position angle. The level of instrumental polarization was <0.1 per cent at all wavelengths. Observations were made through a 4.5 arcsec aperture at the AAT and 12 arcsec at UKIRT. Subtraction of the sky background was achieved by beam switching the telescope. Measurements were made in the following bands:  $U(0.36 \,\mu\text{m})$ ,  $B(0.43 \,\mu\text{m})$ ,  $V(0.55 \,\mu\text{m})$ ,  $R(0.72 \,\mu\text{m})$ ,  $I(0.80 \,\mu\text{m})$ ,

Table 1. The flux and polarization measurements.

OBJECT	DATE & U.T.	WB	FLUX DE			σP (%)	θ (deg)	σθ (deg)
0048-097	20.8.84 17.19 21.8.84 16.28	V R J H B V R J H	1.5 1.9 3.0 5.4 2.5 2.8 3.6 6.5 9.4	0.1 0.2 0.3 0.5 0.2 0.3 0.3 0.6 0.9	27.05 26.01 25.01 23.18 20.15 20.29 19.83 19.77 18.77	0.60 0.56 0.92 0.67 0.38 0.34 0.25 0.39	69.6 69.5 69.2 67.9 56.9 56.7 56.1 54.2	0.6 0.4 1.0 0.8 0.6 0.4 0.4 0.6
(4) (5)	17.8.84 18.24 18.8.84 18.29 20.8.84 18.14	UBVRIJHKRHUBVRJHRHH	8.0 9.7 12.5 16.6 26.4 34.4 40.1 12.5 31.4  6.4 8.1 10.4 15.6 31.4 12.5 31.4	0.7 0.9 1.1 1.5 2.4 3.2 3.7 1.2 2.9  0.6 0.7 1.0 1.4 2.9 1.1 2.9	11.92 10.34 8.75 7.44 7.03 4.52 3.43 2.69 7.24 3.31 14.28 12.42 11.25 9.74 6.33 5.18 10.26 6.12	0.41 0.30 0.22 0.14 0.24 0.11 0.19 0.87 0.17 0.23 0.57 0.23 0.27 0.18 0.38 0.15 0.23	38.4 34.0 35.2 33.7 33.9 32.1 30.8 32.0 37.6 38.0 39.3 40.7 41.5 43.5 43.8 44.6 45.5	0.6 0.6 0.5 1.1 0.8 1.0 8.0 0.8 1.2 1.6 0.7 0.5 1.4
0219+428 (3C66A) (7)	13.8.82 (UKIRT)	R K			10.4 9.7	2.5	34 32	6 5
0235+164	23.12.82	R I J H	1.3 2.4 5.5 9.5	0.1 0.2 0.5 0.9	8.79 5.87 7.58 7.97	1.40 2.00 1.10 0.80	138 133 124 129	5 1 4 3
0420-014	21.8.84	V R H	0.57 0.71 2.3	0.05 0.07 0.2	8.51 11.11 13.43	0.88 0.68 1.00	51.0 55.0 49.1	3.0 1.8 2.0
0521-365 (10)	18.8.84 19.17	R H	2.8 8.6	0.3	2.79 2.98	0.23 0.33	147 135	2.2
0537-441 (11)	23.12.82 13.29	V R J H	1.8 2.2 6.1 9.1	0.2 0.2 0.6 0.8	6.84 7.87 5.78 6.61	0.90 0.70 0.70 0.80	125 132 143 148	4 2 4 4
0548-322 (12)	23.12.82 14.05	R H	1.9	0.2	1.39 0.95	0.80	18 14	13 24
0735+178 (13)	23.12.82 14.18	B V R I J H K	5.6 6.5 9.5 15.3 19.9 23.3	0.5 0.6 0.9 1.4 1.8 2.1	17.56 18.39 18.40 18.59 16.59 16.47 12.16	1.20 0.60 0.30 0.50 0.40 0.40 4.00	1 18 1 14 1 16 1 08 1 16 1 14 1 06	2 1 1 1 1 1 8
0754+101 (0I090.4) (14)	22.12.82 17.45	V R I J H	4.5 4.7 7.3 11.5 15.0	0.4 0.4 0.7 1.1	7.39 7.59 7.38 6.97 6.91	0.46 0.46 0.53 0.42 0.50	30 27 23 28 34	2 2 2 2.4 1.7

742 C. Brindle et al.

## Table 1-continued

OBJECT	DATE & U.T.	WB	FLUX DEN	NSITY (F	F) P (%)	σP (%)	θ (deg) (	σθ deg)
(15)	23.12.82 15.32	V J H	12.4 14.5	1.1	5.61 5.60 4.20	1.0 0.60 1.00	32 32.3 38	5 2.8 7
0818-128 (16)	23.12.82 16.17	R H	1.1	0.1	15.25 17.83	1.20	58 62	3 3.5
0851+202 (0J287) (17)	23.12.82 16.35	B V R I J	5.4 7.7 9.4 12.9 21.8	0.5 0.7 0.9 1.2 2.0	9.77 8.49 9.60 9.98 9.88 9.63	0.70 0.50 0.30 0.60 0.50 0.30	78 71 70 68 77 79	2 1.6 1 1.2 1.4
1514-241 AP LIB (18)	15.8.84 11.56	V R J H	1.7 3.2 5.5 8.3	0.1 0.3 0.5 0.7	4.92 3.22 3.07 3.31	0.59 0.30 0.32 0.44	169 172 175 169	3 2 3 4
(19)	18.8.84	V R I J	3.4 4.6 6.5 5.5	0.3 0.5 0.6 0.5	4.16 3.89 3.21 3.44	0.24 0.23 0.23 0.52	176 173 177 169	1.7 2 2 3 2.4
(20)	21.8.84 11.07	H R H	9.9 5.0 6.8	0.9 0.5 0.6	3.23 3.42 3.27	0.28 0.39 0.65	167 169 179	3   6
1538+149 (21)	21.8.84	B V R H	0.26 0.49 0.64 2.0	0.02 0.05 0.06 0.2	32.82 29.61 29.21 24.76	1.30 0.70 0.95 1.04	128.9 131.3 130.8 129.6	1.1 0.7 1.0- 1.3
1652+398 (MK501) (22)	13.8.82 (UKIRT)	V J K			3.0 4.0 2.7	0.5 1.3 0.7	132.6 126.3 146.8	4.3 11.7 6.6
1749+096 (23)	18.8.84 11.15	V R H	1.3 1.9 5.4	0.1 0.2 0.5	11.24 12.36 13.67	0.49 0.46 0.50	178 0.1 178.6	1.3 1
(24)	19.8.84 10.36 21.8.84 11.13	V R I J H B V R	1.7 2.5 3.4 4.6 7.1 0.95 1.5 2.3	0.15 0.2 0.3 0.4 0.7 0.09 0.1	15.16 14.76 14.83 13.67 13.61 32.00 31.30 29.70	0.36 0.23 0.32 0.36 0.37 0.91 0.56 0.28	160.3 157.6 158.3 160 160.7 146.6 147.8	0.7 0.7 0.8 0.7 0.8 1
		I J H	3.1 4.8 7.1	0.3 0.4 0.6	28.13 24.82 23.04	0.52 0.35 0.51	147.2 147.4 150.7	0.6
1921-293 (26)	19.8.84 10.20	R H	0.71 0.90	0.07 0.08	1.78 7.1	1.31	37 141	14 14
2115-30 (0X-325) (27)	19.8.84 12.52	R H	1.1	0.1	1.56	0.30 3.40	54 162	1 1 7
2128-12 (28)	19.8.84 13.02	R H	2.1	0.2	0.66 2.28	0.38	37 151	13 13
2155-15 (OX-192) (29)	19.8.84 13.10	V R J H	0.37 0.47 0.88 1.4	0.03 0.04 0.08 0.1	32.69 31.57 28.12 26.86	1.29 0.72 1.59 1.35	6.4 6.4 5.1 3.7	0.6 1.7
(30)	21.8.84 13.37	R H	0.50	0.05	31.25	0.77	5.3	0.7

Table 1-c	ontinued			Buzur opucui unu IK poiurizaiion						
OBJECT	DATE & U.T.	WB	FLUX DI (mJy)	ENSITY ( σF	F) P (%)	σP (%)	θ (deg)	σθ (deg)		
2155-304 (31)	16.5.82	B V R I J			7.8 8.0 7.8 7.6 7.7	0.2 0.1 0.1 0.2 0.2	10 9 6 7 12	1 1 1 1		
(32)	17.8.84 12.37	H K U B V R I J	22.4 23.0 25.1 30.7 41.2	2.1 2.1 2.3 2.8 3.8	8.1 10.5 5.49 5.78 5.71 5.38 5.44 4.96	0.2 2.0 0.19 0.10 0.10 0.07 0.09	15 5 165.0 166.2 166.6 167.6 166.9 168.4	1 5 1.1 0.6 0.5 0.4 0.5		
(33)	19.8.84 15.24 21.8.84 12.51	K R H U B V R I J H K	49.3 57.7 9.1 11.3  24.5 25.2 30.2 36.9 49.5 54.1 47.1	4.5 5.3 0.8 1.0  2.3 2.3 2.8 3.4 4.6 5.0 4.3	4.74 5.12 2.15 3.27 3.61 3.88 4.03 3.44 3.99 3.84 4.02 3.33	0.18 0.64 0.30 0.40 0.25 0.13 0.11 0.11 0.06 0.17 0.74	168.8 174.0 21.9 17 37.9 37.0 34.2 34.2 32.9 30.9 32.3 25.0	0.6 3.0 1.8 4 2 0.8 1.1 1.1 0.6 0.6 1.4 5.7		
2200+420 (BL LAC) (35)	13.8.82 (UKIRT)	V R J H			12.5 10.7 8.3 10.0 10.5	1.9 0.8 5.0 1.0 0.6	33 26.0 13.0 24.8 18.4	5 2.3 12.0 3.0 1.8		
2201+044	21.8.84	R H	20.6 18.2	1.9	0.18 1.11	0.16 0.23	119 64	16 6		
2208-137 (37)	21.8.84 13.58	R H	1.1 1.5	0.1 0.1	0.96 4.53	0.32 1.89	16 87	15 14		
2223-052 (3C446) (38)	21.8.84	R H	0.58 2.0	0.05 0.2	1.64 8.50	1.28	147 148	13 10		
2230+115 (CTA102) (39)	21.8.84	V R H	0.79 0.85 1.1	0.07 0.08 0.1	6.74 8.35 11.65	0.85 0.47 2.83	169.7 170.3 171	3.4 1.7 6		
2251+158 (40)	19.8.84 15.07	R H	1.0 1.5	0.09 0.1	2.48 1.79	0.72	160 146	6 19		
2254+074 (0Y+091) (41)	18.8.84 14.36 21.8.84 15.55	B V R J H V R	0.57 0.78 0.99 1.9 3.0 0.78 1.2 2.8	0.05 0.07 0.09 0.2 0.3 0.07 0.1	20.4 17.62 15.36 13.24 12.69 20.45 17.71 12.40	1.0 0.56 0.51 0.51 0.72 0.45 0.37 0.94	54.5 54.8 55.2 53.7 53.6 54.9 54.1	1.4 0.9 0.9 1.3 1.5 0.7 0.5		
2345-167 (43)	21.8.84 16.24	R H	0.19 0.45	0.02 0.04	1.87	1.85	22	45		

A summary of all the polarization and flux density data is given in Table 1, and Fig. 1(a)-(h) shows the data for those objects where there is good wavelength coverage and repeat observations were made. Plots of the data for some other objects are presented in Fig. 3(a)-(n), which also has model fits superimposed (see Sections 4.1-4.3). In Table 2 we present for each

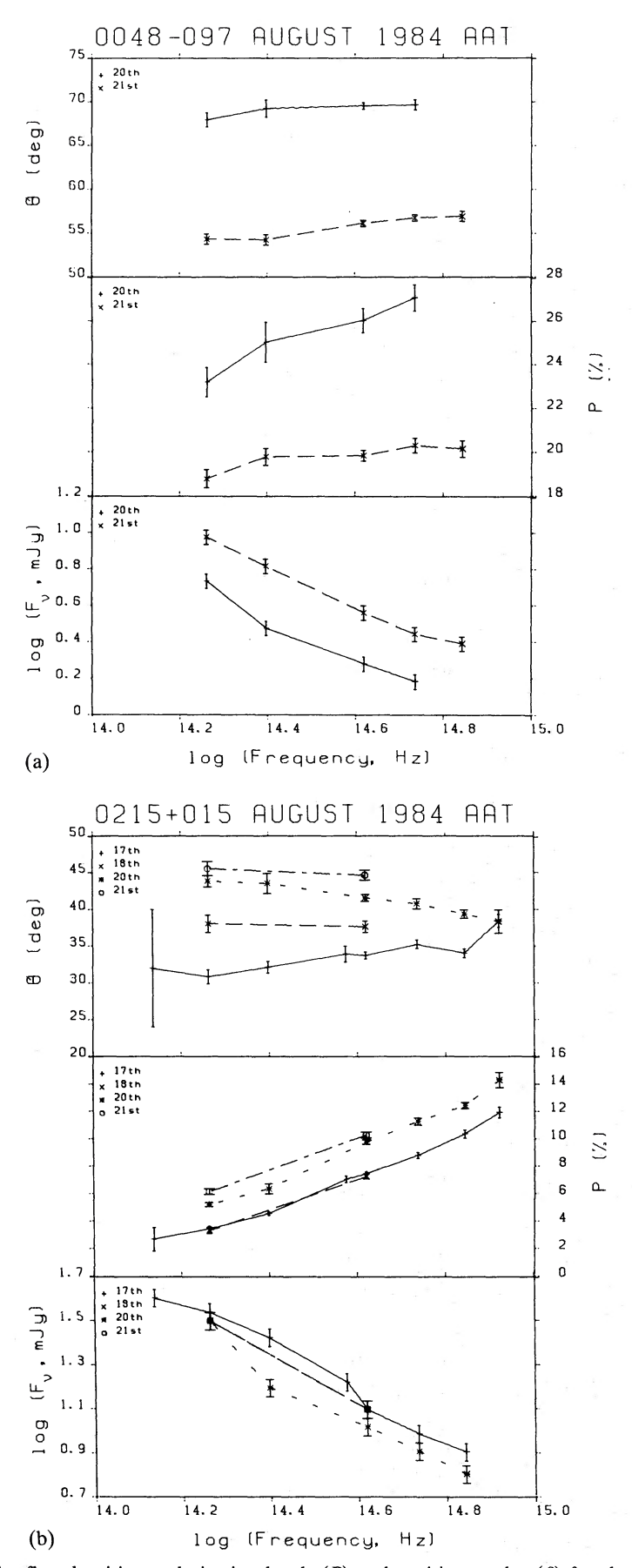
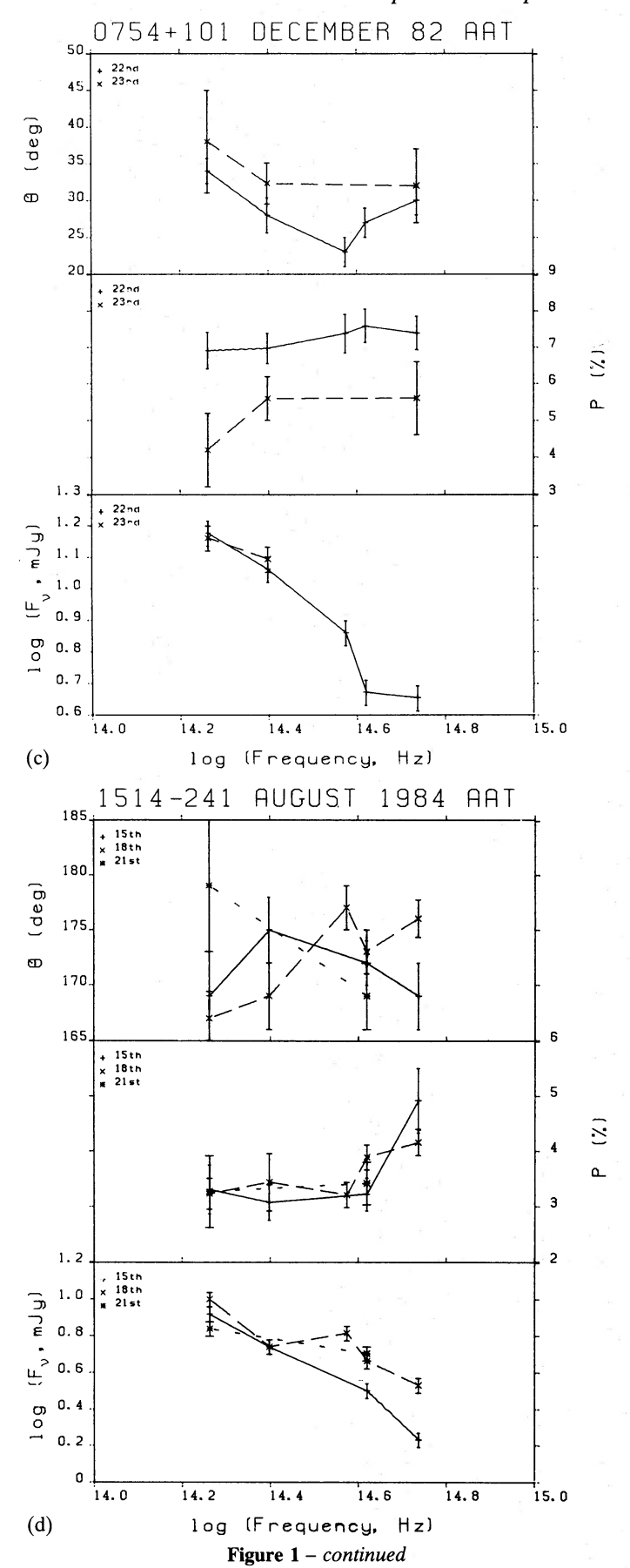
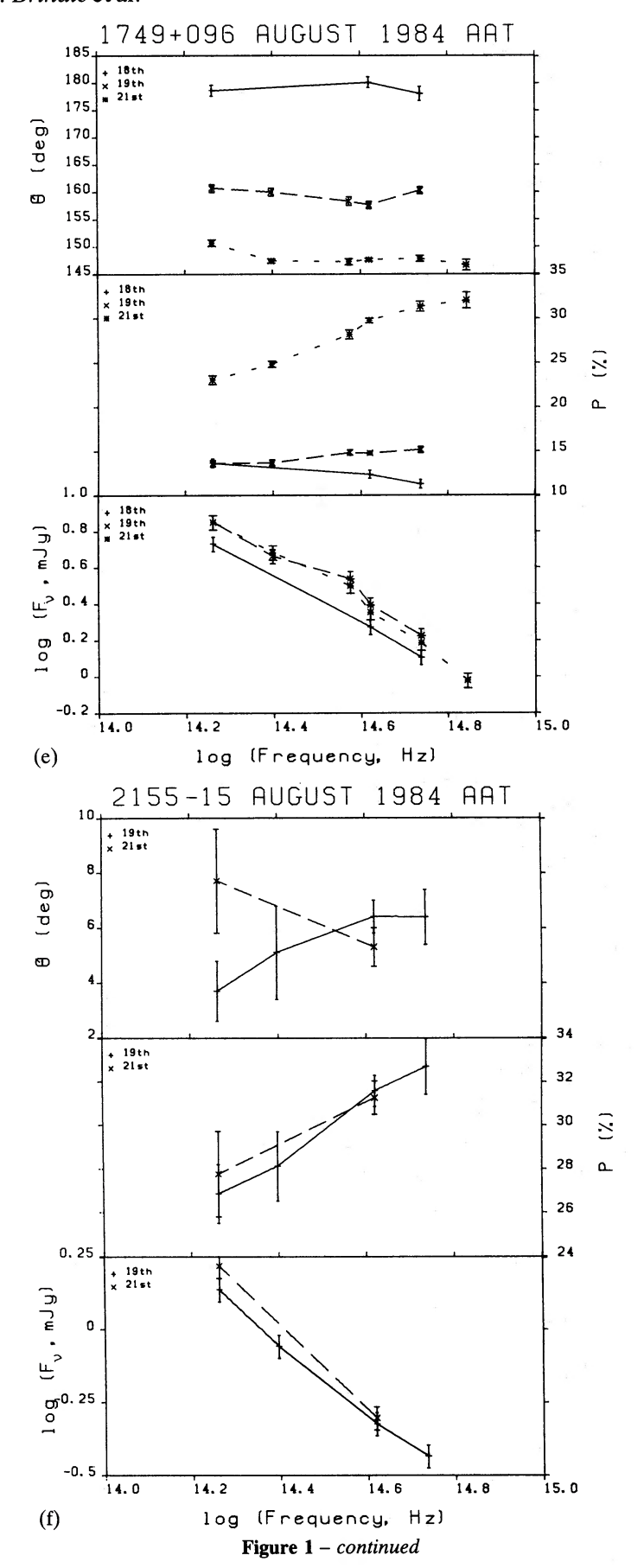
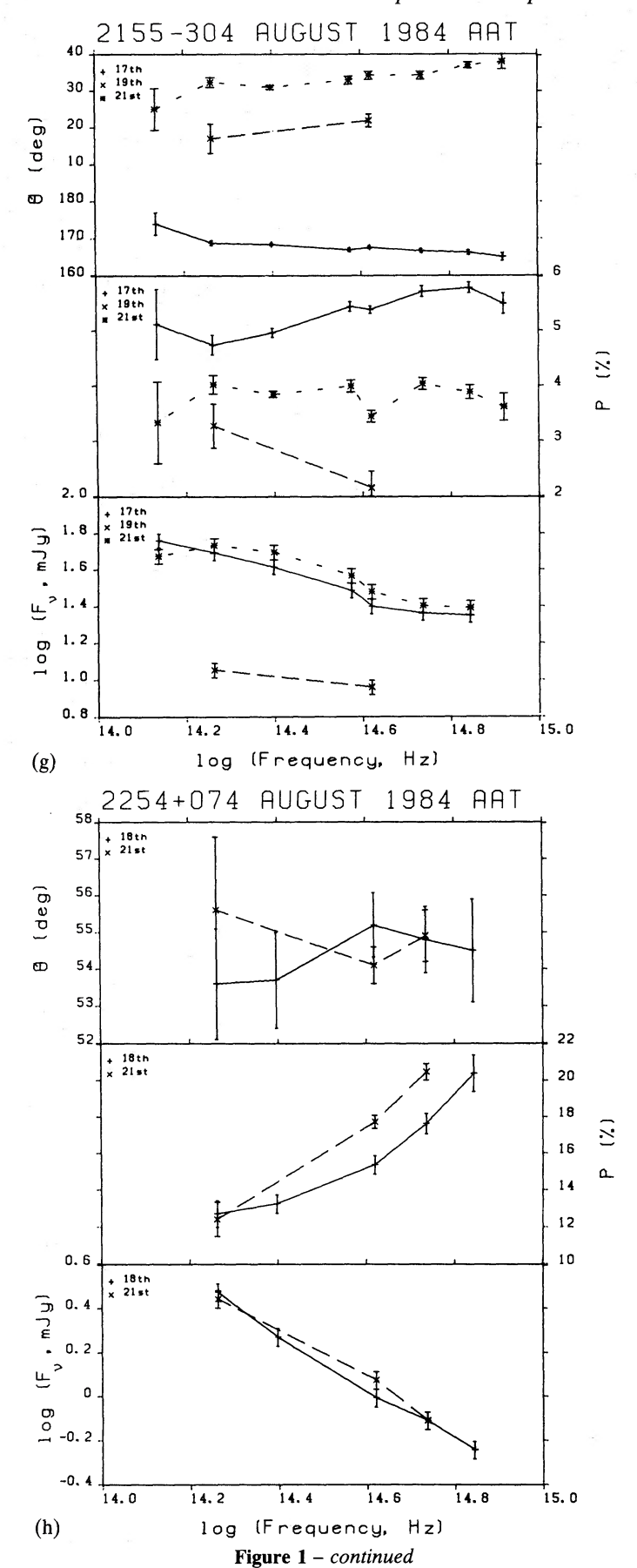


Figure 1. (a)-(h) The flux densities, polarization levels (P) and position angles  $(\theta)$  for those blazars that were observed on more than one occasion.







object its redshift and a list of references, dated from 1980, of optical, infrared and radio polarization studies. The review by Angel & Stockman (1980) gives information on some of the objects and references to earlier polarization studies. The fluxes presented are those calculated after the magnitudes have been corrected for interstellar extinction using the E(B-V) values from Burstein & Heiles (1982) and the reddening curves of Whitford (1958) and Willner & Pipher (1983) for  $\lambda < 1 \, \mu \text{m}$  and  $\lambda > 1 \, \mu \text{m}$ , respectively. The absolute flux calibration of Bessell (1979) and that presented by Ward *et al.* (1982) was used to compute the optical and infrared fluxes respectively. The degree of polarization has been corrected for noise bias (Wardle & Kronberg 1974). No correction for interstellar polarization has been made, since most objects lie well away from the galactic plane.

**Table 2.** A summary of the redshift of each object and references to earlier polarization studies.

OBJECT	TYPE	REDSHIFT	OPTICAL	REFERENCES INFRARED	RADIO
0048-097	BL		27		8,28
0215+015	BL	1.254a,1.345a 1.549a,1.649a & 1.686a	1,27	1,2	28
0219+428	BL	0.444u	1,27	1,2	23,28
0235+164	BL	0.524a,0.524 & 0.852a	1,4,6 27	2,4	8,9,14,15,21, 28
0420-014	ovv	0.633,0.915	17		9,14,28
0521-365	BL	0.055	1	1	20,23
0537-441	BL	0.894			24
0548-322	BL	0.069			
0735+178	BL	0.424	7,27	2,3,7	14,28
0754+101	BL		1,7,27,29	1,2,7	14,23,28
0818-128	BL		27	3	28
0851+202	BL	0.306a	5,11,27	2,5	9,14,15,21,23, 28
1514-241	BL	0.049			28
1538+149	ВĹ		6	3	28
1652+398	BL	0.034		3	10,23,28
1749+096	BL				8,9,14,21, 28
1921-293	BL	0.353		4	28
2115-30	BL	0.980			
2128-123	QSO	0.501	18,19		
2155-15	BL				28
2155-304	BL	0.170			23
2200+420	BL	0.069	1,6,7,12, 13,27,30	1,2,3,7	9,10,14,16,21,23, 28

Table 2 - continued

OBJECT	ТҮРЕ	REDSHIFT	OPTICAL	REFERENCES INFRARED	RADIO	
2201+044	BL	0.028				
2208-137	OVV	0.392	17,18,19			
2223-052	ovv	0.847a,1.404	17,27		14,21,28	
2230+114	ovv	1.037	17		21,26,28	
2251+158	OVV	0.859	17,18,19,		21,22,25,26, 28	
2254+074	ovv	1	27		20	
2345-167	ovv	0.600	17			

BL=BL Lac, QSO=quasar, OVV=OVV quasar u denotes uncertain redshift, a denotes absorption redshift

#### References

(1)	Bailey <i>et al</i> . 1984.
(2)	Holmes et al. 1984a.

- (3) Impey et al. 1984.
- (4) Impey et al. 1982.
- (5) Holmes *et al.* 1984b.
- (6) Wills et al. 1980.
- (7) Puschell *et al.* 1983.
- (8) Altschuler 1980.
- (9) Aller et al. 1981.
- (10) Rudnick & Jones 1982.
- (11) Kulshrestha et al. 1984.
- (12) Moore et al. 1982
- (13) Brindle et al. 1985.
- (14) Rudnick et al. 1985.
- (15) Roberts et al. 1984.

- (16) Aller & Aller 1984.
- (17) Moore & Stockman 1981.
- (18) Moore & Stockman 1984.
- (19) Stockman et al. 1984.
- (20) Wardle et al. 1984.
- (21) Barvainis & Predmore 1984.
- (22) Cotton et al. 1984.
- (23) Aller et al. 1982.
- (24) Komesarof et al. 1982.
- (25) Cotton et al. 1982.
- (26) Simard-Normandin et al. 1981.
- (27) Sitko et al. 1985.
- (28) Aller et al. 1985.
- (29) Marchenko 1985.
- (30) Hagen-Thorn et al. 1985.

# 3 Statistical properties of the data

## 3.1 OCCURRENCE OF WAVELENGTH DEPENDENCE

Weighted least-squares regression lines have been fitted to the polarization data, and the gradients  $(dP/d\lambda)$  and  $d\theta/d\lambda$  are summarized in Table 3. Also included are the computed spectral indices  $(F \propto \lambda^{\alpha})$  and the rest-frame luminosities at V. The latter are calculated using these spectral indices, and adopting  $H_0 = 75 \,\mathrm{km \, s^{-1} \, Mpc^{-1}}$  and  $q_0 = 1$ . Unfortunately, because polarization measurements can be, and often were, made in poor photometric conditions the flux values and hence the spectral indices have relatively large errors. We have not, for example, presented the spectral indices in the optical and infrared separately, since the difference is nearly always less than the associated errors. A steepening of the spectral index with decreasing wavelength (e.g. Cruz-Gonzalez & Huchra 1984) is not, however, inconsistent with our data. From Table 3 it is seen that there is a wavelength dependence of polarization (>3 $\sigma$ ) on 15 occasions, and a wavelength dependence of position angle also on 15 occasions, out of a total 42 observations. The data also show that the phenomenon is a transient one, occurring occasionally in some objects and being absent at other times. It is also seen that some objects display a wavelength dependence in which the polarization in the infrared is higher than that in the optical. This occurs mainly for

Table 3. Some properties of the flux and polarization data.

OBJECT	DATE	SPECTRAL INDEX (α) (F <sub>λ</sub> αλα)		REST-FI LUMINOS AT 0.5	SITY 5 um	dP/dλ (% μm		d0/d (deg	λ ± μm <sup>-</sup> 1)
				(Watts H	Z X	1023)			
0048-097	20.8.84 21.8.84	0.89 1.13	0.35 0.26	7.9 15		-3.32 -1.06		-1.50 -2.49	0.83 0.56
0215+015	17.8.84 18.8.84	1.06 1.12	0.14 0.37	700 900		-5.55 -4.27		-4.80 0.43	0.73 1.57
	20.8.84	0.86	0.27	590		-5.76	0.18	3.64	0.75
	21.8.84	1.12	0.36	900		-4.50	0.34	0.98	1.33
0219+428	13.8.82					-0.48	1.98	-1.36	5.31
0235+164	22.12.82	1.89	0.39	9.3		0.14	1.53	-6.84	3.54
0420-014	21.8.84	1.31	0.25	11		3.71	1.14	4.56	2.60
0521-365	18.8.84	1.36	0.40	0.17		0.21	0.44	-13.04	3.87
0537-441	23.12.82	1.60	0.26	32		-1.10	0.94	19.87	4.24
0548-322	23.12.82	1.44	0.40	0.17		-0.48	1.57	<b>-4.3</b> 5	29.66
0735+178	23.12.82	1.11	0.18	21		-2.21	0.46	0.38	1.07
0754+100	22.12.82	1.20	0.24	24		-0.61		6.18	2.09
0010 120	23.12.82 23.12.82	0.50 1.09	0.93	65 5 <b>.</b> 8		-1.13 2.80		3.54 4.35	7.20 5.01
0010-120	23.12.02	1.09	0.40	9.0					3.01
0851+202	23.12.82	1.21	0.24	10		0.29	0.37	7.80	1.20
1514-241	15.8.84	2.3	0.9	0.082		-0.59		1.16	3.90
	18.8.84 21.8.84	1.3 0.37	0.9 0.37	0.16 0.24		-0.70 -0.16		-8.64 10.87	2.52 7.29
	21.0.04	0.37	0.57	0.24		0.10	0.02	10.07	7.27
1538+149	21.8.84	1.49	0.21	2.6		-5.14	1.07	-0.61	1.26
1652+398	13.8.82					-0.17	0.52	8.36	4.79
1749+096	18.8.84	1.30	0.25	6.8		1.94		-0.50	1.29
	19.8.84	1.25 1.48	0.24	8.9 7.9		-1.53 -8.04		1.56 2.09	0.86 0.57
2115-30	19.8.84	0.11	0.34	24				117.39	
2155-15	19.8.84 21.8.84	1.23 1.41	0.21	1.9		-5.49 -3.78		-2.68 2.61	1.20 2.20
2155 207									
2155-304	16.5.82 17.8.84	0.64	0.45	1.3		-0.87	0.18	4.98 2.47	0.96 0.51
	19.8.84	0.26	0.35				0.54		4.77
	21.8.84	0.51	0.15	15		0.04	0.11	-5.51	0.93
2200+420	8.82					-0.34	0.63	-5.81	1.83
2201+044	21.8.84	-0.15	0.37	0.32		1.01	0.30	-59.8	18.6
2208-137	21.8.84	0.38	0.32	3.5		3.88	2.08	77.2	22.3
2223-052	21.8.84	1.50	0.37	28		7.46	3.59	1.09	17.8
2230+115	21.8.84	0.31	0.26	19		5.04	2.64	1.07	6.23
2251+158	19.8.84	0.49	0.31	16		<b>-0.</b> 75	2.42	-15.2	21.7
2254+074	18.8.84 21.8.84	1.24 1.14	0.26 0.29			-5.22 -7.23			1.33 1.93
2345-167	21.8.84	1.05	0.39	1.5					

low-redshift BL Lacs, when the optical polarization is less than about 10 per cent, and for OVV quasars in which this behaviour has been noted before (e.g. Moore & Stockman 1981, 1984).

#### 3.2 SPECTRAL DEPENDENCE OF POLARIZATION

Bailey, Hough & Axon (1983, hereafter BHA) first noted that the polarization in blazars at shorter (optical) wavelengths was generally greater than that at longer (infrared) wavelengths, and this dependence increased with increasing polarization. HBIW reached a similar conclusion based on their infrared data. To further examine this dependence we present in Fig. 2(a) a plot of the polarization at  $H(1.64 \,\mu\text{m})$  against the polarization at  $R(0.72 \,\mu\text{m})$ . The solid, diagonal line corresponds to wavelength-independent polarization, and the dashed line to a linear regression fit to all the data in the Fig. 2(a). To aid identification of a particular object in the figure, the number alongside the data points corresponds to the number in brackets in Table 1. This plot shows the following features:

- (i) The data for the majority of objects are consistent with no wavelength dependence, (see also Section 3.1). However, for the entire data set a linear regression fit, taking into account errors in both coordinates, gives  $P_H = (0.83 \pm 0.05) P_R 0.2 \pm 0.1$  at the 95 per cent confidence limit.
- (ii) A few objects display significant wavelength dependence, in which the polarization usually decreases with increasing wavelength. From Table 3 it is seen that these objects are amongst the most luminous ones in the sample.
- (iii) Contrary to the findings of BHA and HBIW, wavelength dependences with  $dP/d\lambda < 0$  occurred for both small ( $P \lesssim 10$  per cent) and large polarizations ( $P \gg 10$  per cent), and therefore the correlation of increasing wavelength dependence with increasing polarization is weaker.
- (iv) The infrared polarization can be greater than that in the optical for levels of optical polarizations <10 per cent this same feature can be seen in the data of BHA and HBIW.

A wavelength dependence of position angle in blazars has been found to be a rare occurrence (e.g. BHA), with usually no more than a few degrees rotation between the optical and infrared, although large rotations have been observed in some BL Lacs (e.g. Holmes *et al.* 1984b; Sitko *et al.* 1984). In Fig. 2(b) we present a plot of the position angle at *H* against the position angle at *R*. Again, in this figure, the solid, diagonal line corresponds to wavelength-independent position angle. This diagram shows that only a few objects have any significant wavelength dependence of position angle.

### 3.3 GALAXY DILUTION

Dilution from a host galaxy will reduce the observed level of polarization and this reduction will itself be wavelength dependent. For example, the galaxy flux of giant elliptical galaxies like NGC 4486, thought to be the host galaxies of BL Lacs (e.g. Weistrop 1982), peaks at about  $1.3\,\mu\mathrm{m}$  and decreases rapidly to shorter wavelengths (Grasdalen 1980; Lebofsky 1980) in the galaxy's rest frame. Consequently, when such a spectrum is redshifted the flux density will decrease much more rapidly in the optical than in the infrared. Objects with large redshifts and for which polarization measurements have been made will tend to have particularly luminous cores dominating the overall emission, and hence galaxy dilution will be unimportant.

To examine how galaxy dilution can affect the measured polarization at different redshifts, we have used the K-corrections tabulated in Coleman et al. (1980), and the galaxy colours for different redshifts from Lilly & Longair (1982) to calculate the galaxy contribution relative to the total blazar flux. At a redshift of z = 0.05 we assumed different values of the ratio of the galaxy flux to total flux at V, and then computed the galaxy flux at other redshifts by taking  $q_0$  to be 1. The

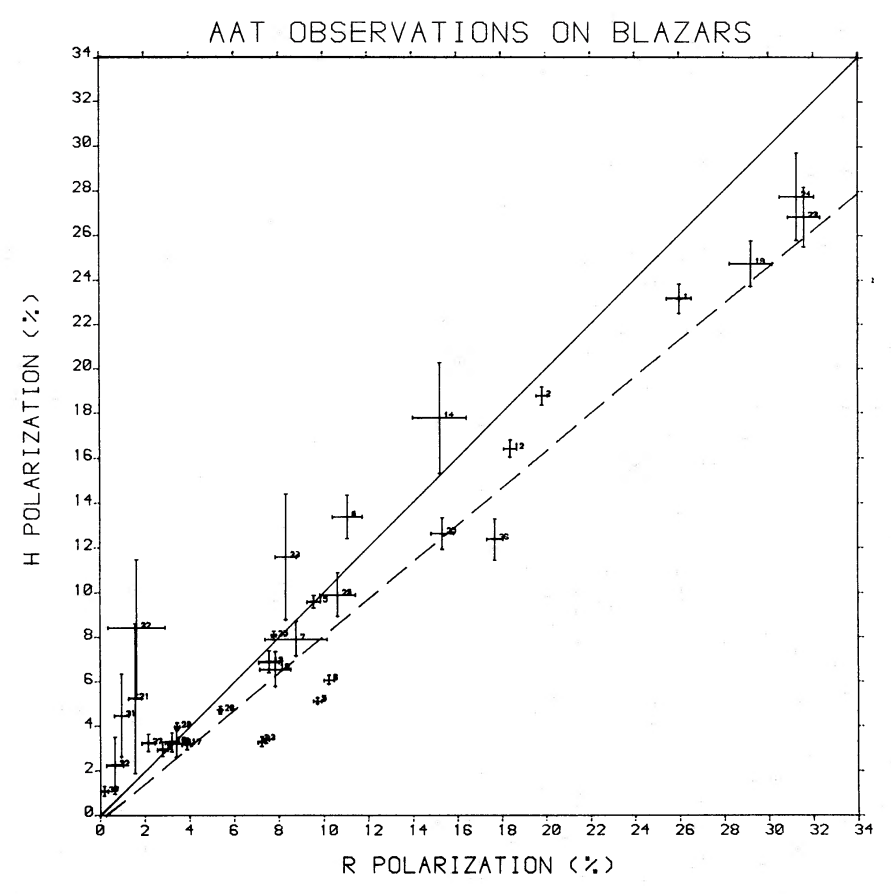


Figure 2. (a) Polarization level at H plotted against that at R. The dashed line is a regression line fit to all the data.

non-thermal flux of the blazar core was computed for different values of the spectral index; these values also being used to compute the non-thermal flux at other redshifts. In this simple model we assumed that the intrinsic polarization of the blazar is wavelength independent and that there is no galaxy polarization. Although we can draw the following conclusions from our calculations, we emphasize that making accurate corrections for galaxy dilution is difficult since for individual objects the contribution from the galaxy is very uncertain:

- (i) The value of the ratio, R, of the observed polarization at V to that at K is most sensitive to the spectral index,  $\alpha$ , of the non-thermal source. For small values of  $\alpha$ , a significant wavelength dependence of polarization results even when the galaxy contribution at V is small (5 per cent).
- (ii) Since the value of R is independent of the intrinsic polarization level, the wavelength dependence will be most noticeable when the intrinsic polarization is high.

Six of our objects have redshifts less than 0.1 (see Table 2), and for these objects galaxy dilution may be important. We note, however, that all have similar optical and infrared polarizations, suggesting that galaxy dilution is not in fact important. An exception is 2201+044, which has the lowest redshift of our sample and an optical polarization very much larger than that in the infrared, even though its overall polarization is very low.

#### 4 Models

## 4.1 SINGLE-COMPONENT MODELS

Various models have been proposed to explain the wavelength dependence of polarization observed in some blazars.

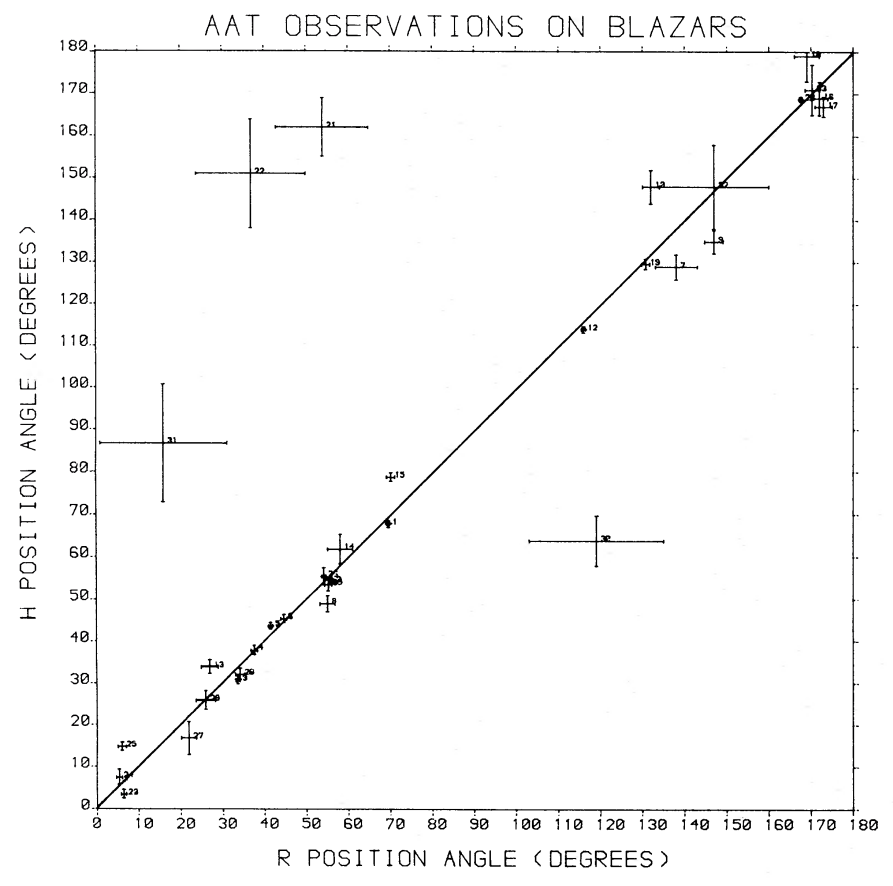


Figure 2. (b) Polarization position angle at H plotted against that at R.

The spectral polarization of optically thin synchrotron emission from relativistic electrons gyrating in a uniform magnetic field was first investigated by Westfold (1959). Nordsieck (1976) calculated the polarization from a power-law electron distribution with a sharp high-energy cut-off, for several specific magnetic field distributions. For small polarizations he found that the polarization could be described as a function of local spectral index, for a given magnetic field distribution. Björnsson & Blumenthal (1982) considered the polarization of optically thin synchrotron emission from an arbitrary magnetic field distribution. An important result from their work is that the polarization can either increase or decrease as a function of the local spectral index, depending on whether the field alignment increases or decreases with field strength, respectively.

Recently Björnsson (1985) has shown how strong wavelength dependent polarization (in both the degree and position angle) can be produced by a single source, even when the spectral index changes only by a small amount. This arises if the relative contributions to the flux originating in different parts of the source, possessing different polarization properties, change with wavelength. Björnsson discusses two extreme cases of a particular source geometry, which produce the following polarization characteristics:

- (i) Strong wavelength dependence of degree of polarization, with a corresponding wavelength dependence of position angle.
- (ii) Strong wavelength dependence of degree of polarization, without a wavelength dependence of position angle.

In the first case Björnsson shows that  $dP/d\lambda$  is negative and the maximum polarization change is a factor of 2 for  $\Delta \log \nu \sim 1$ . Changes in position angle accompany the changes in polarization,

754

with larger changes in the former occurring in steeper spectra. In the second case Björnsson shows how larger changes of polarization with wavelength can arise without a corresponding position angle rotation.

Björnsson suggests that multicomponent models, as discussed in detail in Section 4.3 of this paper, may be approximations to a single very complex synchrotron component. We note, however, that changes in polarization with wavelength greater than the maximum of a factor 2 predicted by Björnsson for case (1), do occur (e.g. 0215+015, this paper).

In this paper, we have not attempted to model the data using single complex synchrotron sources of the type discussed by Björnsson (1985). Instead we have considered synchrotron models in which the polarization is only a function of the spectral index (e.g. Nordsieck 1976; Björnsson & Blumenthal 1982), and is independent of the electron and magnetic field distributions. There is now good evidence that in most blazars a power-law spectrum in the optical and near-infrared regions, is only a first approximation to a spectrum that gradually steepens with decreasing wavelength, with the spectral index increasing by about 0.5 from the optical to the infrared (e.g. Allen, Ward & Hyland 1982; Cruz-Gonzalez & Huchra 1984; Worrall et al. 1984). If the field alignment increases with field strength, then a wavelength dependence of polarization will result with  $dP/d\lambda < 0$ . Hence small changes in the level of polarization between the optical and infrared can be accounted for by such a single synchrotron source provided there is a significant change in the spectral index between the two regions.

We have considered a model consisting of a single synchrotron component, with an emission spectrum of the form

$$S = k\lambda^a \exp(-b \log^2 \lambda),$$

where k, a and b are constants. When b is zero the spectrum is of a power-law form with spectral index, a, and when it has a negative value it produces a convex-shaped spectrum with the spectral index increasing with decreasing wavelength. The polarization is given by

$$P = c(\alpha + 1)/(\alpha + \frac{5}{3})$$

where  $\alpha$  is the local spectral index and c the magnetic field alignment parameter, being 1 for a perfectly uniform field and 0 when it is completely random. We calculate that a single source with the spectral index decreasing from 1.0 to 0.5 between the optical and infrared, will produce an optical polarization about 10 per cent higher than that in the infrared. A 15 per cent change can be produced if the spectral index decreases from 1.0 to 0.25. Although reasonable model fits can be obtained to some objects with such modest wavelength dependences, unfortunately the data are not accurate enough to constrain them. However, this type of single source cannot account for a wavelength dependence of position angle, unless Faraday rotation is responsible, which we discuss briefly in the next section.

We have also considered another model based on monoenergetic electron injection into a magnetic field. The emission spectrum is given by

$$S = k\lambda^{1/2} \exp(-\lambda_0/\lambda),$$

where k and  $\lambda_0$  are constants, (Falla & Evans 1975). For those objects which can be modelled by a single synchrotron source, we find equally acceptable fits using either emission spectrum.

#### 4.2 FARADAY ROTATION

Although Faraday rotation is unlikely to be important at optical and near-infrared wavelengths, it has in fact been suggested as a possible cause of some large polarization position angle rotations seen occasionally in some objects (e.g. Rieke *et al.* 1977; Puschell *et al.* 1983).

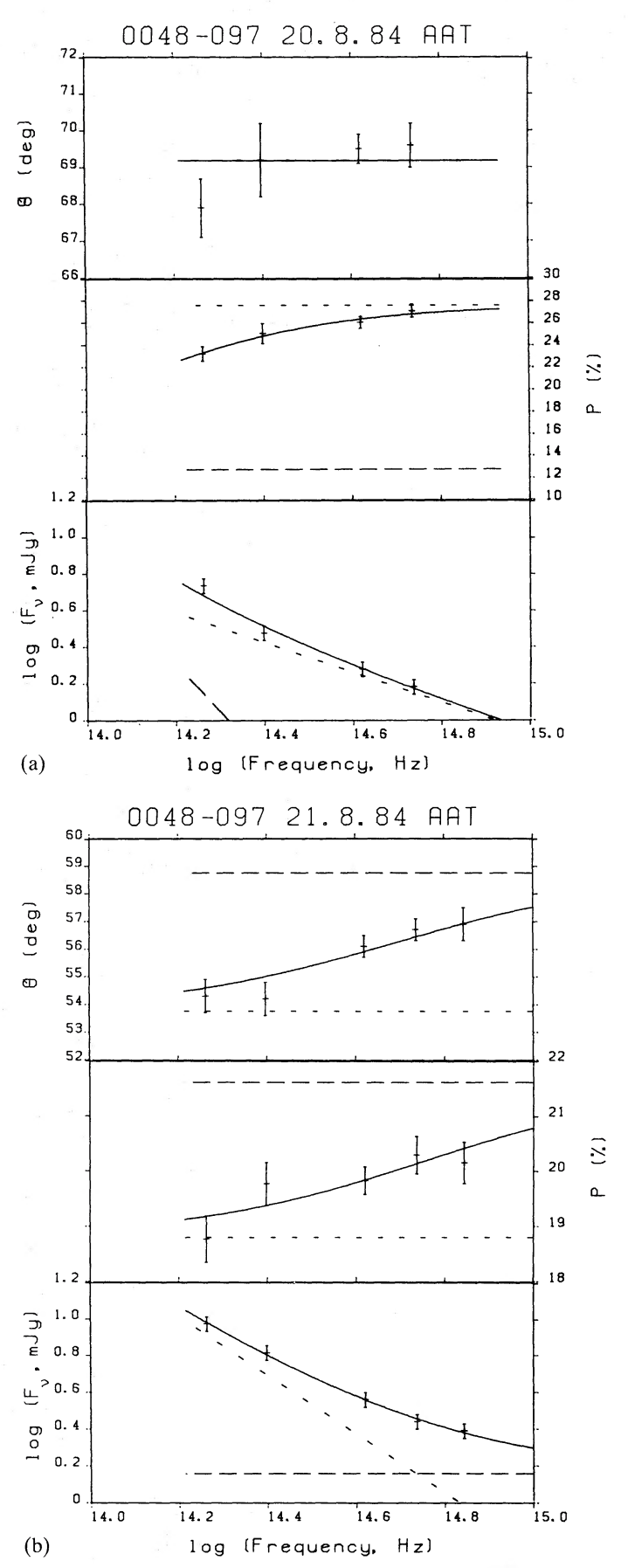
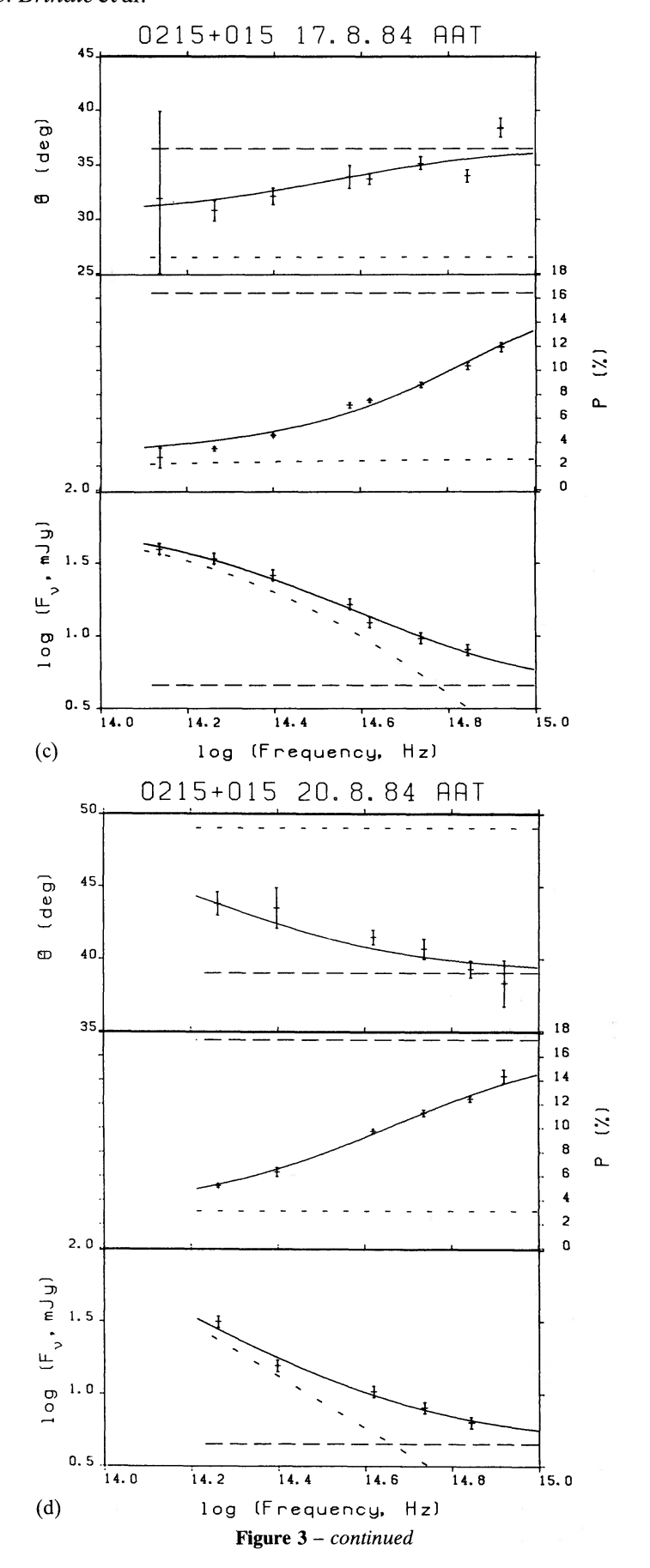
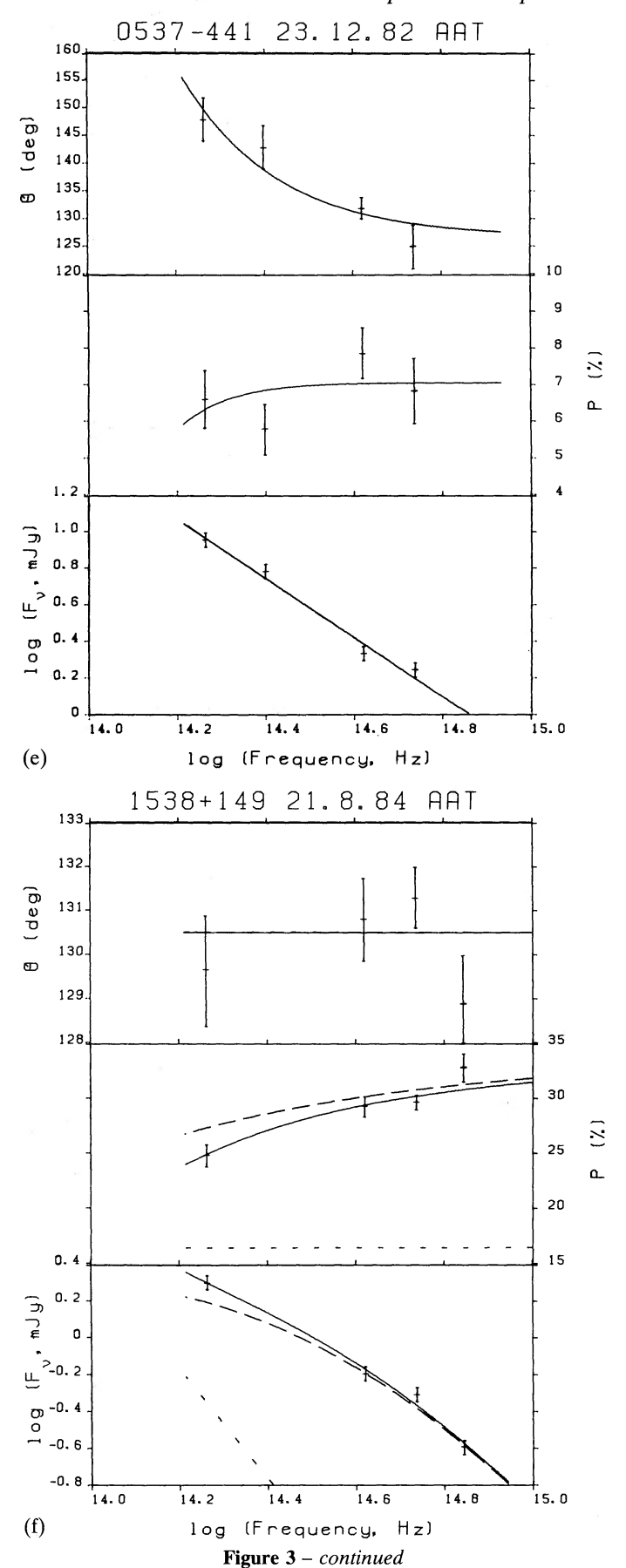
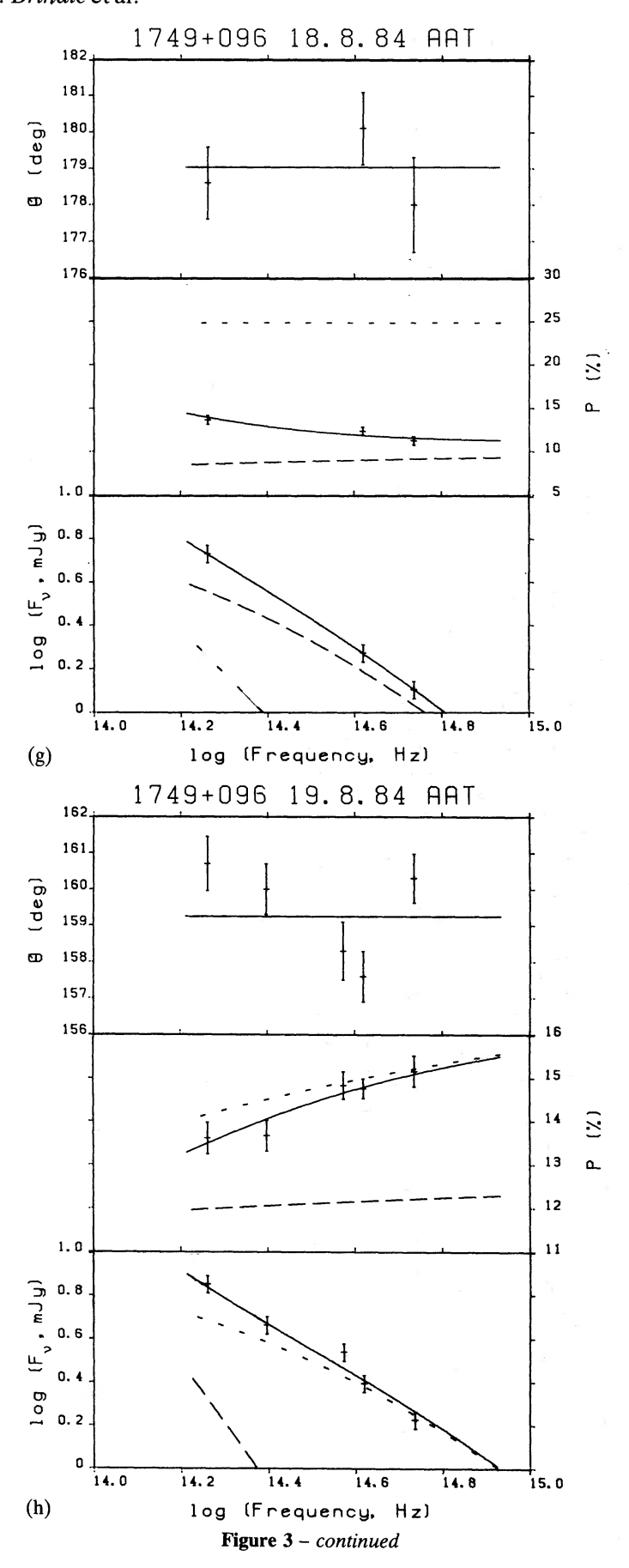
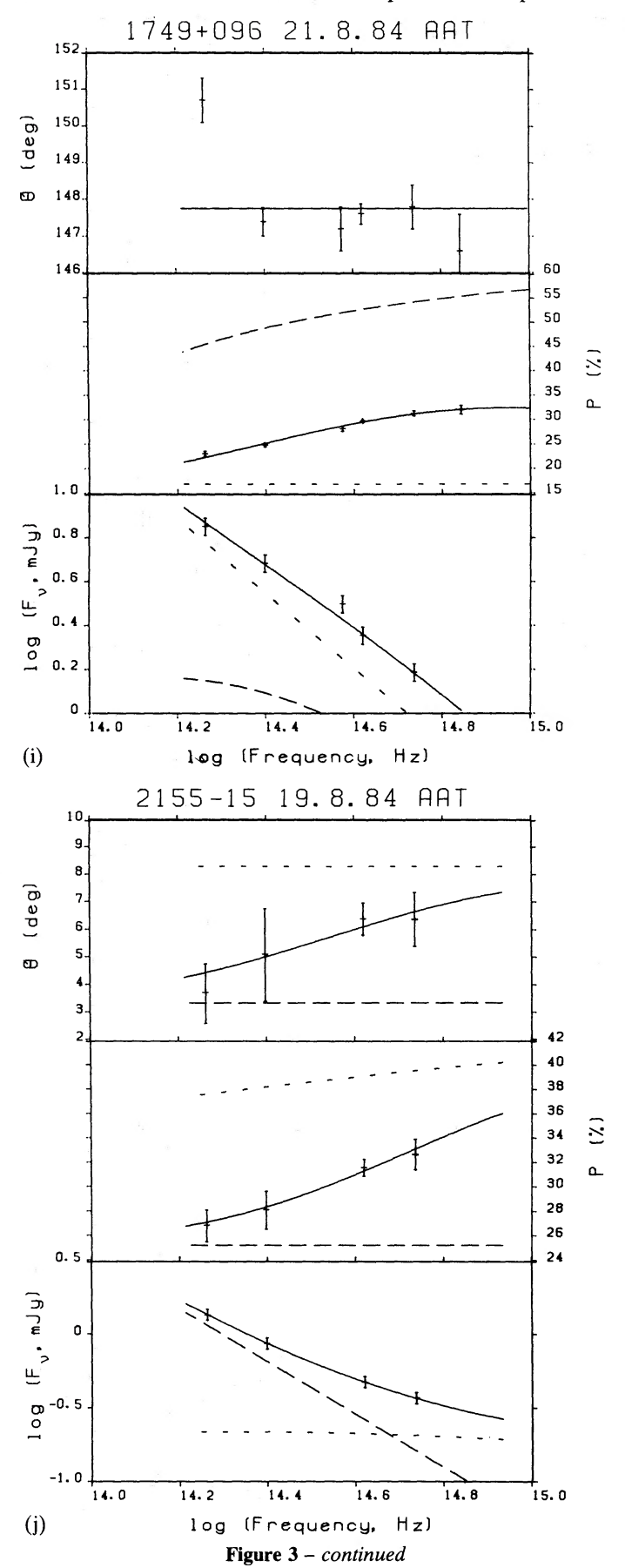


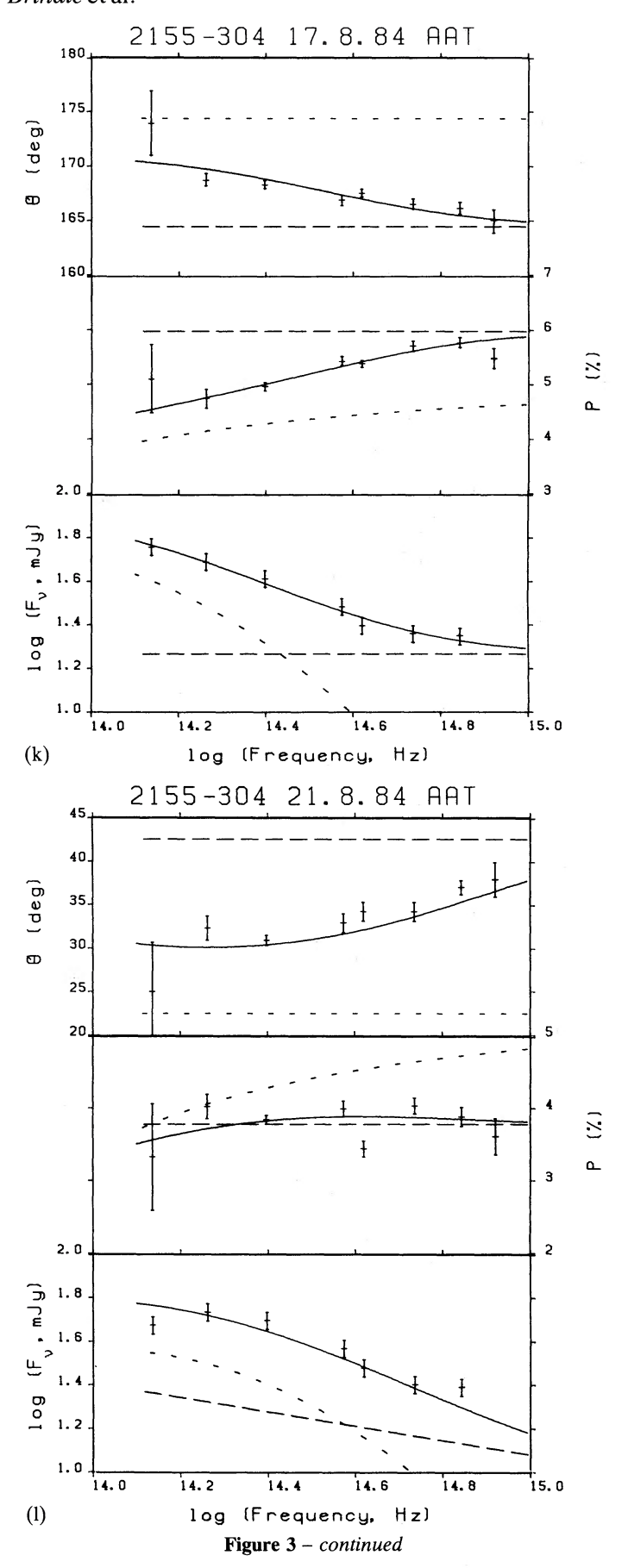
Figure 3. (a)–(n) The model fits discussed in Section 4.4. The solid lines represent the resultant flux, polarization and position angle due to the superposition of the two sources indicated by dashed lines.

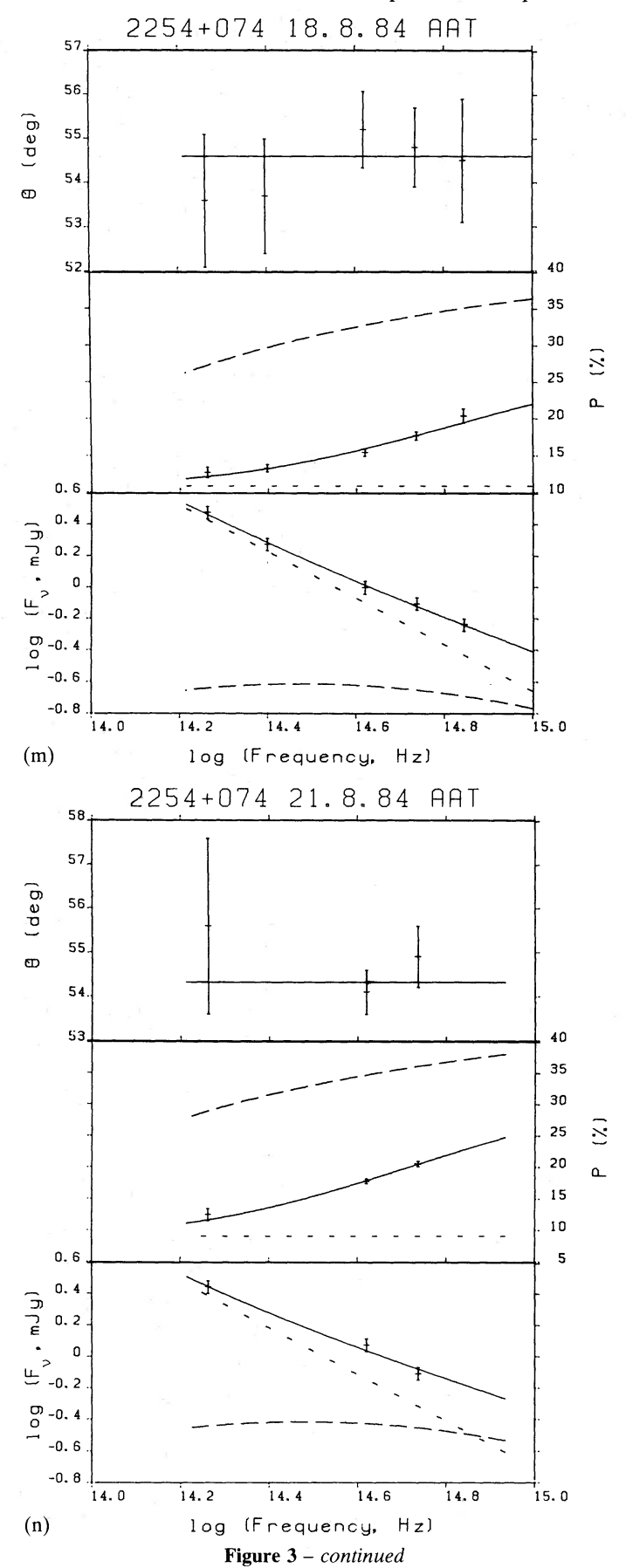












We have made least-squares fits to our data for the case of a synchrotron source of the first type discussed in Section 4.1, and included Faraday rotation with the source geometry of a cylinder whose axis is parallel to the line-of-sight (a jet seen end-on) using the formulae presented by Cioffi & Jones (1980). For most objects the model fits are unsatisfactory, since the rotation measures deduced from the variation of position angle with wavelength are too small to produce the necessary wavelength dependence of polarization. The only exception is 0537-441 (see Fig. 3e) in which a large rotation of position angles is observed, but the errors in the polarization are too large to constrain the model sufficiently.

#### 4.3 TWO-COMPONENT MODELS

Although one of the simple synchrotron sources, considered in the previous section, cannot account for the wavelength dependence of polarization in most of the objects, since the observed spectral curvature is too small, two or more sources with different spectra and polarizations can produce a great diversity of polarization behaviour. Such models have been successfully applied to other polarization data showing a wavelength dependence (e.g. Puschell et al. 1983; Holmes et al. 1984b). Such a model can also account for a wavelength dependence of position angle if the sources have different polarization position angles.

We have made least-squares fits to the data using a model consisting of two of the synchrotron sources first discussed in Section 4.1. The resultant polarization of the two sources is given by,

$$P = P_1(1+X^2Z^2+2ZX\cos 2\Delta\theta)^{1/2}/(1+X)$$

where  $X=S_2/S_1$ ,  $Z=P_2/P_1$  and  $S_1$ ,  $S_2$ ,  $P_1$  and  $P_2$  are the fluxes and polarizations respectively of the two sources at a particular wavelength;  $\Delta\theta$  is the difference between the position angle of polarization of the first source,  $\theta_1$ , and the second one,  $\theta_2$ . The resultant position angle is given by,

$$\theta = 0.5 \arctan \left[ (\sin 2\theta_1 + ZX \sin 2\theta_2) / (\cos 2\theta_1 + ZX \cos 2\theta_2) \right].$$

The parameters  $k_1$ ,  $k_2$ ,  $a_1$ ,  $a_2$ ,  $b_1$  and  $b_2$  were first obtained from a least-squares fit to the flux data, and then  $c_1$ ,  $c_2$ , and  $\Delta\theta$  from a fit to the polarization levels, and, finally,  $\theta_2$  from a fit to the position angles. Several iterations, in which the flux parameters were varied slightly from the initial value, were necessary to obtain acceptable fits to the (more accurate) polarization data.

Satisfactory fits to most objects with large wavelength dependences have been obtained with this model. A few general features of the model fits are apparent, these being:

- (i) The component with the flattest flux distribution usually has the highest polarization. This is clearly necessary for  $dP/d\lambda$  to be negative.
- (ii) Some of the individual sources still require large changes in spectral index between the optical and infrared so that the sources themselves have strong wavelength dependences.

We have also made least-squares fits to a model consisting of two sources each having an injection of monoenergetic electrons of the type discussed in Section 4.1. This model produces fits that are about as good as the ones produced by the model described earlier in this section. More accurate flux data would be necessary to distinguish between the two different source spectra.

To conclude this section we note that Sitko, Stein & Schmidt (1984) and Björnsson (1985, see also Section 4.1) have argued that multiple-component models are inapplicable, unless the components are in some way physically coupled. However, monitoring of the optical polarization of BL Lac by Moore *et al.* (1982) and Brindle *et al.* (1985) has shown that the variability is consistent with a multicomponent model. For 0215+015, although we cannot definitely rule out a single synchrotron source of the type discussed by Björnsson (1985), we believe that a two-component model adequately accounts for the data.

#### 4.4 MODEL FITS

In this section reference to single-component models, except where otherwise specified, refers to synchrotron models in which polarization is a function of the spectral index only (see Section 4.1 for further details).

#### 4.4.1 0048-097

Our observations between 1984 August 20–21 (see Fig. 1a) show a large increase in the flux ( $\sim$ 100 per cent), a decrease in the levels of polarization by around 5 per cent, and an anticlockwise rotation of position angles ( $\sim$ 15°). On the August 20 there is marginal wavelength dependence of polarization ( $dP/d\lambda < 0$ ) and no wavelength dependence of position angles. On August 21 there is also a marginal wavelength dependence of polarization, of the same form but smaller magnitude, and a marginal wavelength dependence of position angles with an anticlockwise rotation of a few degrees from the optical to the infrared.

A single synchrotron component poorly fits the data on August 20 and can be ruled out on August 21 when there is a wavelength dependence of position angle. A two-component model can, however, fit the data reasonably well on both occasions (see Fig. 3a and b).

#### $4.4.2 \ 0.215 + 0.15$

Our observations between the 1984 August 17–21 (see Fig. 1b) show an increase in the levels of polarization, by about 2 per cent, and a clockwise rotation of position angle with the infrared position angles rotating by about 15° and the rotation decreasing with decreasing wavelength. A strong wavelength dependence of polarization was present on all occasions with  $dP/d\lambda < 0$ , and this spectral dependence remained the same in all four days of observations. During this period the flux underwent only small variations.

A single synchrotron component model can be ruled out (see Section 4.1), but two components can satisfactorily fit the data on August 17 and 20, when there is sufficient wavelength coverage (see Fig. 3c and d). Changes in flux are not large enough to explain the changes in polarization and rotations of position angles, but they can be accounted for by a rotation of the source dominating the emission in the infrared, together with changes in the magnetic field configuration of the other component.

### 4.4.3 0537-441

Our observations show polarization levels consistent with an absence of wavelength dependence, but a clockwise rotation of position angles of 25° from the optical to the infrared. A Faraday rotation model fit is shown in Fig. 3(e).

## 4.4.4 1538+149

Our observations show high levels of polarization together with a strong wavelength dependence  $(dP/d\lambda < 0)$ . The two-component model fit is shown in Fig. 3(f).

#### 4.4.5 1749 + 096

Our observations (see Fig. 1e) show dramatic polarization variability. Between the August 18–19 the flux increased by  $\sim$ 40 per cent and the polarization levels by  $\sim$ 4 per cent at V with decreasing

#### 764 *C. Brindle* et al.

magnitude towards longer wavelengths, and underwent an anticlockwise rotation of position angles ( $\sim$ 10°). On August 18 there is a marginal wavelength dependence of polarization with  $dP/d\lambda < 0$  and the position angles are wavelength independent. On August 19 there is a marginal wavelength dependence of polarization with  $dP/d\lambda < 0$  and a marginal wavelength dependence of position angle with a few degrees clockwise rotation between the optical and infrared. Between the August 19–21 the flux levels remained approximately constant, whilst the level of polarization increased by about 15 per cent in the optical and 10 per cent in the infrared, and the position angles rotated anticlockwise by about 10°. The wavelength dependence of polarization became stronger and the position angles are again marginally wavelength dependent.

The data suggest that a new synchrotron component was 'switching-on' and steadily increasing in polarization and brightness between August 18-21. A second component with an intrinsic polarization of about 10 per cent in the optical is necessary to account for the wavelength dependence of polarization. In Fig. 3(g)-(i) we show the model fits.

# 4.4.6 2155-15

Our observations in the 1984 August 19–21 (see Fig. 1f) show high levels of polarization, together with a strong wavelength dependence  $(dP/d\lambda < 0)$ . On August 19 there is a marginal wavelength dependence of position angles. Between the two dates there are no significant changes in flux and polarization. The strong wavelength dependence is satisfactorily modelled by two synchrotron components (see Fig. 3j).

#### 4.4.7 2155-304

Our observations between 1984 August 17–21 (see Fig. 1g) show changes in flux, polarization and position angles over the four days. Between August 17–19 the flux declined by about 90 per cent, the polarization levels decreased by about 3 per cent, and the position angles rotated clockwise by about 30°. On August 17 there is a marginal wavelength dependence of polarization  $(dP/d\lambda < 0)$  and a marginal wavelength dependence of position angle  $(d\theta/d\lambda < 0)$ . Between August 19–21 the flux increased to just above its initial levels in August 17, the polarization levels increased by about 1 per cent, and the position angles rotated by about another 10°. This object displayed an unusually flat flux spectrum on all three occasions. On August 21 there is no wavelength dependence of polarization (to within the errors) and a marginal wavelength dependence of position angles  $(d\theta/d\lambda < 0)$ .

The flux and polarization changes are best accounted for by assuming two synchrotron components are present. The model fits are shown in Fig. 3(k) and (l).

#### 4.4.8 2254 + 074

Our observations on 1984 August 18 and 21 (see Fig. 1h) show high levels of polarization, together with a strong wavelength dependence  $(dP/d\lambda < 0)$ . Between the two dates there is an increase in the optical polarization levels by about 2 per cent without any significant changes in the flux levels or position angles. In Fig. 3(m) and (n) we show the model fits.

#### 4.5 INTERPRETATION OF THE SPECTRAL DEPENDENCE OF POLARIZATION

To illustrate how the wavelength dependence phenomenon can be explained by a two-component model, we have re-plotted our data (see Fig. 4) in the same form presented by BHA and superimposed curves for various parameters of the model discussed in Section 4.3. The curves

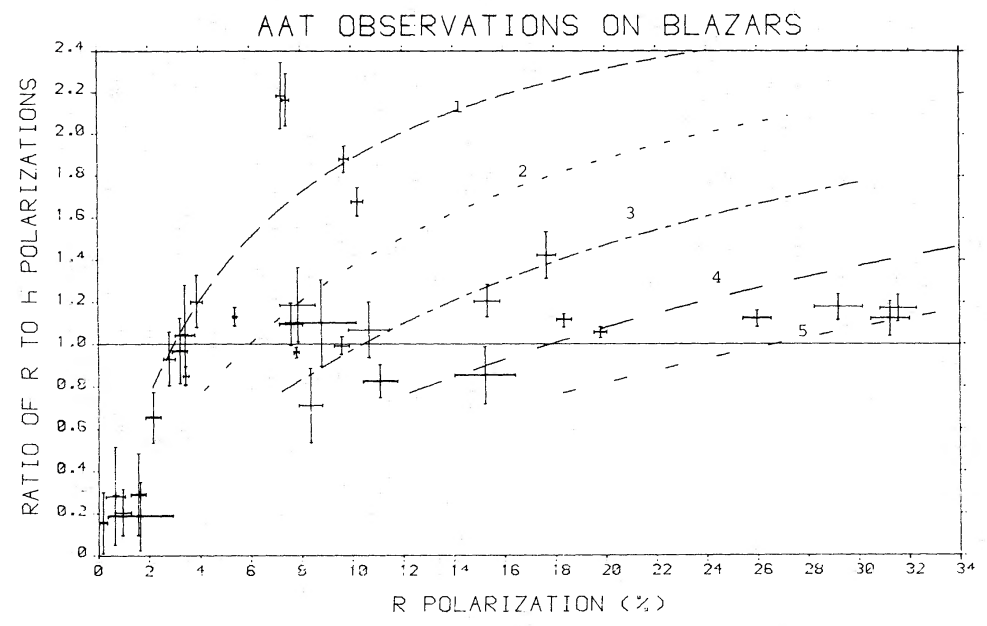


Figure 4. The ratio of R to H polarization plotted against the polarization at R. Curves 1–5 correspond to values of  $c_2$  of 0.04, 0.08, 0.14, 0.20 and 0.26, respectively, and the parameter values listed in Section 4.5.

have been computed for the following parameters;  $a_1=0$ ,  $a_2=1.5$ ,  $b_1=b_2=-0.228$ ,  $\lambda_0=0.5 \,\mu\text{m}$ ,  $c_1=0$  to 1. The differences in the curves is entirely due to the different values of  $c_2$  (0.04, 0.08, 0.14, 0.20 and 0.26). The values of  $b_1$  and  $b_2$  give a change in spectral index of 0.5 between 0.5 and 1.5  $\mu$ m.  $\lambda_0$  is the wavelength at which the total fluxes of the two sources are equal.

It can be seen (Fig. 4) that the two-component model can easily reproduce a wide variety of wavelength dependences. We can infer that the maximum polarization of the infrared component is usually about 15 per cent. Even though infrared polarizations may reach 30 per cent or more, the intrinsic polarization of the infrared component need only be around 15 per cent. Larger polarizations can be produced by a suitable combination of component parameters.

#### 4.6 POSSIBLE SOURCE LOCATIONS

Blazars are thought to be active galactic nuclei (AGNs) in which relativistic jets play an important role. In particular, BL Lacs are believed to be AGNs with jets seen nearly end-on, and OVV quasars AGNs with jets at larger angles to the line-of-sight (e.g. Blandford & Königl 1979; Marscher 1980; Königl 1981; Königl & Choudhuri 1985a). In the former case the beamed jet emission is believed to overwhelm any other emission component, whereas in the latter objects the emission from the central power-house itself might be important. The highly variable, steep-spectrum, optical emission of blazars might then be associated with the inner, optically emitting region of a jet, where the magnetic field is more ordered and consequently the polarization higher. Marscher (1980) points out that in this region the development of thermal instabilities in the fluid flow is promoted, and short-term fluctuations could be produced with time dilation shortening the variability time-scale in the observer's rest frame. In contrast, emission from the central power-house region will have a fairly flat spectrum and the highly disordered magnetic field, thought to exist there, will give rise to a low polarization, as observed in the 'normal' quasars (e.g. Stockman et al. 1984). Moore & Stockman (1981), from a consideration of the emission-line equivalent widths, concluded that in OVV quasars the anisotropic jet emission dominates, typically contributing 70-80 per cent of the continuum.

OVV quasars sometimes display a wavelength dependence with the polarization increasing with increasing wavelength. This can possibly be accounted for by the superposition of the jet component and central component.

One of the main characteristics of the observations reported here, is the general constancy of position angle with wavelength. Consequently, in the two-component model discussed in Section 4.3, both components must have closely aligned position angles, indicating they originate in a region, or regions, with the same magnetic field orientation. This suggests that both components are most likely located in the inner region of a jet. One component could be associated with the relatively steady jet emission and the other, more variable component, with the various instabilities which arise in the jet flow. This model is similar to that presented by Holmes *et al.* (1984b) to interpret some complex behaviour of OJ287, although in their model the two components had very different position angles.

Rotations of position angles, as seen in 0215+015, can be interpreted as either a physical rotation of a magnetic field, or a change in magnetic field configuration along a jet as a shock propagates in the fluid flow (e.g. Königl & Choudhuri 1985b). Changes in the level of polarization in individual components can arise from local changes in the ordering of the field. We note that a simple two-component model can produce large polarization changes, without accompanying large changes in flux, as is often observed for blazars. This is an advantage compared to the relativistic aberration models (Björnsson 1982) in which, because of Doppler boosting, polarization changes are accompanied by large flux changes (Björnsson 1982; Brindle *et al.* 1985). HBIW also concluded, from their large data base infrared photometry and polarimetry, that the variability of BL Lacs is consistent with a model consisting of at least two variable, polarization components.

A somewhat different scenario is that discussed by Brindle *et al.* (1985) for BL Lacs, in which they suggest that the total emission arises both from flaring on an accretion disc and an underlying constant source, which might be associated with the jet. The flaring could be the precursor stage to the injection of relativistic electrons into a jet, as discussed by Pineault (1981). Different relative contributions from the jet and the accretion disc account for the differences in polarization behaviour of BL Lac as described by Moore *et al.* (1982) and that decribed by Brindle *et al.* (1985), for two different 'monitoring runs' of several weeks duration. The latter authors found the position angle of polarization for BL Lac varied only slightly from a mean angle of 28° and suggested that the main emission originated in the jet. This was in contrast to the large and apparently chaotic variations in position angle reported by the former authors when BL Lac was about three times brighter. At this epoch Brindle *et al.* (1985) conclude that the high variability resulted from flaring on an accretion disc with each source having random position angles, as might be expected close to the central engine where magnetic fields are expected to be chaotic. Unfortunately, in both 'monitoring runs' of BL Lac, little, or no, spectral information was available, and therefore models similar to those presented in this paper could not easily be tested.

It is clear that in order to better determine the nature of the synchrotron sources in blazars (i.e. number of independent sources, location in a jet or accretion disc), detailed wavelength dependent information, as well as temporal coverage, is essential.

#### 5 Conclusions

The polarization data presented in this paper have shown that for the majority of objects the wavelength dependence of polarization is relatively low with, on average, the level of polarization in the infrared less than that in the optical by 10 to 20 per cent, and with no more than a few degrees rotation of position angle. Much larger wavelength dependences were observed amongst the more luminous objects in the sample, e.g. 0215+015. The data have also shown that large

wavelength dependences can occur for both large (P>10 per cent) and small ( $P \le 10$  per cent) values of the optical polarization, contrary to previous findings.

The observed wavelength dependences of both the flux and polarization can in all cases be well modelled by the superposition of two synchrotron sources with different spectra and magnetic field alignment parameters. In some cases inter-day variability can be ascribed to a high-polarization variable source together with a relatively quiescent low-polarized source.

# Acknowledgments

We thank PATT and ATAC for the allocation of observing time at UKIRT and the AAT. CB thanks Hertfordshire County Council for a LEA Research Assistantship. We also thank the staff at AAO and UKIRT for assistance at the telescope. Dr. C-I. Björnsson is thanked for clarifying some points on his single-component synchrotron model.

#### References

Allen, D. A., Ward, M. J. & Hyland, A. R., 1982. Mon. Not. R. astr. Soc., 199, 969.

Aller, H. D. & Aller, M. F., 1984. In: VLBI and Compact Radio Sources, IAU Symp. No. 110, p. 119, eds Fanti, R., Kellermann, K. & Setti, G., Reidel, Dordrecht, Holland.

Aller, H. D., Aller, M. F. & Hodge, P. E., 1981. Astr. J., 86, 325.

Aller, M. F., Aller, H. D. & Hodge, P. E., 1982. In: Extragalactic Radio Sources, IAU Symp. No. 97, p. 335, eds Heeschen, D. S. & Wade, C. M., Reidel, Dordrecht, Holland.

Aller, H. D., Aller, M. F., Latimer, E. & Hodge, P. E., 1985. Astrophys. J. Suppl. Ser., 59, 513.

Altschuler, D. R., 1980. Astr. J., 85, 1559.

Angel, J. R. P. & Stockman, H. S., 1980. Ann. Rev. Astr. Astrophys., 18, 321.

Angel, J. R. P. et al., 1978. In: Pittsburgh Conference on BL Lac Objects, p. 117, ed. Wolfe, A. M., University of Pittsburgh Press.

Bailey, J. & Hough, J. H., 1982. Publs astr. Soc. Pacif., 94, 618.

Bailey, J., Hough, J. H. & Axon, D. J., 1983. Mon. Not. R. astr. Soc., 203, 339.

Barvainis, R. & Predmore, C. Read, 1984. Astrophys. J., 282, 402.

Bessell, M. S., 1979. Publs astr. Soc. Pacif., 91, 589.

Björnsson, C-I., 1982. Astrophys. J., 260, 855.

Björnsson, C-I., 1985. Mon. Not. R. astr. Soc., 216, 241.

Björnsson, C-I & Blumenthal, G. R., 1982. Astrophys. J., 259, 805.

Blandford, R. D. & Königl, A., 1979. Astrophys. J., 34.

Brindle, C. et al., 1985. Mon. Not. R. astr. Soc., 214, 619.

Burstein, D. & Heiles, C., 1982. Astr. J., 87, 1165.

Cioffi, D. F. & Jones, T. W., 1980. Astr. J., 85, 368.

Coleman, G. D., Wu, C-C. & Weedman, D. W., 1980. Astrophys. J. Suppl. Ser., 43, 393.

Cotton, W. D., Geldzahler, B. J. & Shapiro, I. I., 1982. In: Extragalactic Radio Sources, p. 301, eds Heeschen, D. S. & Wade, C. M., Reidel, Dordrecht, Holland.

Cotton, W. D., Geldzahler, B. J., Macaide, J. M., Shapiro, I. I., Sanroma, M. & Rius, A., 1984. Astrophys. J., 286, 503.

Cruz-Gonzales, I. & Huchra, J. P., 1984. Astr. J., 89, 441.

Falla, D. & Evans, A., 1975. Astrophys. Space Sci., 37, 11.

Grasdalen, G. L., 1980. In: Objects of High Redshift, IAU Symp. No. 92, p. 269, eds Abell, G. O. & Peebles, P. J. E., Reidel, Dordrecht, Holland.

Hagen-Thorn, V. A., Marchenko, S. G. & Yakovleva, V. A., 1985. Astrofizika, 22, 5.

Holmes, P. A., Brand, P. W. J. L., Impey, C. D. & Williams, P. M., 1984a. Mon. Not. R. astr. Soc., 210, 961. Holmes, P. A. et al., 1984b. Mon. Not. R. astr. Soc., 211, 497.

Impey, C. D., Brand, P. W. J. L., Wolstencroft, R. D. & Williams, P. M., 1982. Mon. Not. R. astr. Soc., 200, 19.

Impey, C. D., Brand, P. W. J. L., Wolstencroft, R. D. & Williams, P. M., 1984. Mon. Not. R. astr. Soc., 209, 245.

Komesaroff, M. M., Milne, D. K., Rayner, P. T., Roberts, J. A. & Cooke, D. J., 1982. In: *Extragalactic Radio Sources*, p. 331, eds Heeschlen, D. S. & Wade, C. M., Reidel, Dordrecht, Holland.

768 C. Brindle et al.

Königl, A., 1981. Astrophys. J., 243, 700.

Königl, A. & Choudhuri, A. R., 1985a. Astrophys. J., 289, 173.

Königl, A. & Choudhuri, A. R., 1985b. Astrophys. J., 289, 188.

Kulshrestha, A. K., Joshi, U. C. & Deshpande, M. R., 1984. Nature, 311, 733.

Lebofsky, M. J., 1980. In: Objects of High Redshift, IAU Symp. No. 92, p. 257, eds Abell, P. O. & Peebles, P. J. E., Reidel, Dordrecht, Holland.

Lilly, S. J. & Longair, M. S., 1982. Mon. Not. R. astr. Soc., 199, 1053.

Marchenko, S. G., 1985. Astrofizika, Vol. 22, No. 1, p. 15.

Marscher, A. P., 1980. Astrophys. J., 239, 296.

Martin, P. G., 1985. In: Active Galactic Nuclei, ed. Dyson, J. E., University of Manchester Press.

Moore, R. L. & Stockman, H. S., 1981. Astrophys. J., 243, 60.

Moore, R. L. & Stockman, H. S., 1984. Astrophys. J., 279, 465.

Moore, R. L. et al., 1982. Astrophys. J., 260, 415.

Nordsieck, K. H., 1976. Astrophys. J., 209, 653.

Pineault, S., 1981. Astrophys. J., 246, 612.

Puschell, J. J., Jones, T. W., Phillips, A. C., Rudnick, L., Simpson, E., Sitko, M., Stein, W. A. & Moneti, A., 1983. Astrophys. J., 265, 625.

Rieke, G. H., Lebofsky, M. J., Kemp, J. C., Coyne, G. V. & Tapia, S., 1977. Astrophys. J., 218, L37.

Roberts, D. H., Roberts, R. I., Wardle, J. F. C., Rogers, A. E. E. & Burke, B. F., 1984. In: VLBI and Compact Radio Sources, IAU Symp. No. 110, p. 35, eds Fanti, R., Kellermann, K. & Setti, G., Reidel, Dordrecht, Holland.

Rudnick, L. & Jones, T. W., 1982. Astrophys. J., 255, 39.

Rudnick, L., Jones, T. W., Aller, H. D., Aller, M. F., Hodge, P. E., Owen, F. N., Fiedler, R. L., Puschell, J. J. & Bignell, R. C., 1985. Astrophys. J. Suppl. Ser., 57, 693.

Simard-Normandin, M., Kronberg, P. P. & Button, S., 1981. Astrophys. J. Suppl. Ser., 46, 239.

Sitko, M. L., Schmidt, G. D. & Stein, W. A., 1985. Astrophys. J. Suppl. Ser., 59, 323.

Sitko, M. Stein, W. A. & Schmidt, G. D., 1984. Astrophys. J., 282, 29.

Stockman, H. S., Moore, R. L. & Angel, J. R. P., 1984. Astrophys. J., 279, 485.

Ward, M., Allen, D. A., Wilson, A. S., Smith, M. G. & Wright, A. E., 1982. Mon. Not. R. astr. Soc., 199, 953.

Wardle, J. F. C. & Kronberg, P. P., 1974. Astrophys. J., 194, 249.

Wardle, J. F. C., Moore, R. L. & Angel, J. R. P., 1984. Astrophys. J., 279, 93.

Weistrop, D., 1982. In: Extragalactic Radio Sources, p. 377, eds Heeschen, D. S. & Wade, C. M., Reidel, Dordrecht, Holland.

Westfold, K. C., 1959. Astrophys. J., 130, 241.

Whitford, A. E., 1958. Astrophys. J., 107, 102.

Willner, S. P. & Pipher, J. L., 1983. Astrophys. J., 265, 760.

Wills, D., Wills, B. J., Breger, M. & Hsu, J-C. 1980. Astr. J., 85, 1555.

Worrall, D. M. et al., 1984. Astrophys. J., 284, 512.